



Energy transfer-enhanced external power conversion efficiency in blended polymeric thin film solar devices

Nazir Mustapha¹ · Mohamad S. AlSalhi^{2,3} · Saradh Prasad^{2,3}

Received: 17 October 2018 / Accepted: 8 March 2019 / Published online: 14 March 2019
© Springer Science+Business Media, LLC, part of Springer Nature 2019

Abstract

In this paper, the spectral and electrical properties of a conjugated polymer poly [(9, 9-dioctyl-2, 7-divinylene-fluorenylene)-alt-co-(1, 4-phenylene)] (PFO–MEH–PPV) with poly[3-(2-ethyl-isocyanato-octadecanyl) thiophene] (PECOD) in thin films have been studied. First, PFO–MEH–PPV and PECOD were dissolved in tetrahydrofuran and chloroform respectively for different concentrations. These solutions were deposited on glass substrates to form thin films with different thicknesses. The absorbance and photoluminescence spectra for each individual pure polymer were recorded and contrasted with those for blended conjugated polymer's films to determine the effect of blending on the absorption and photoluminescence. Finally, we present a study on the processing and characterization of organic solar cells fabricated by spin coating pure PFO–MEH–PPV, PECOD and their blend as the organic active layer onto indium tin oxide layer (150 nm), followed by the evaporation of silver cathode (110 nm). The current–voltage characteristics of these cells were determined and external quantum efficiency. Upon blending the two polymers in solid forms, it could be seen that the efficiency (6.25%) for the cells based on a blend layer is higher than the ones without blending (4.4%). Finally, we demonstrated here that the combination/blending of conjugated polymers has resulted in optimized solar device function, with reasonably quantum efficiency higher than 10%.

1 Introduction

In the last two decades, organic conjugated polymers have been widely used in electronics and optoelectronics, including photovoltaic cells [1–5], thin film transistors [6, 7], and light-emitting diodes (LEDs) [8–15]. Electroluminescence (EL) in the conjugated polymers was first reported by Burroughes et al. in 1990 for the fabrication of LEDs [8]. Since then, many researchers have examined the morphology, physical, optical and photoelectric properties of the spin-coated emissive conjugated polymers [10, 11, 16–20]. For LED applications, the polymer used must have two basic

characteristics: electrical conductivity (semiconducting polymer) and high photoluminescence (PL) efficiency [21]. Thus, scientists have focused on improving the absorption and PL characteristics of the conjugated polymers in ultra-violet and visible ranges.

To improve the performance, efficiency, and reliability of optoelectronic devices, researchers have used different kinds of electrodes, inserted more layers between electrodes, and blended polymers to tune their physical properties [3, 5]. The resultant blend can have combined attractive features of the conjugated polymers or new properties that are not present in either of the polymers. Thus, this attractive approach of forming active semiconducting layers in the photovoltaic device by blending conjugated polymers can result in optimized device function, efficiency and lifetime [1].

The recent progress made in improving and up-grading the efficiency of organic solar cells based on conjugated polymers was done by incorporating emissive materials, such as nanoparticles, quantum dots or graphene to the active layer of the devices based on conjugated polymers [22, 23].

According to Mustapha et al. the polymeric cell's photoconductivity increases when electron transport materials ZnO nanoparticles are incorporated into the cells [23]. Different materials such as quantum dots and graphene have

✉ Nazir Mustapha
nmmustapha@imamu.edu.sa

¹ Department of Physics, College of Science, Imam Mohammad Ibn Saud Islamic University, P.O. Box 90950, Riyadh 11623, Saudi Arabia

² Department of Physics and Astronomy, College of Science, King Saud University, P.O. Box 2455, Riyadh 11451, Saudi Arabia

³ Research Chair on Laser Diagnosis of Cancers, College of Science, King Saud University, P.O. Box 2455, Riyadh 11451, Saudi Arabia

been used to improve the performance of organic solar cells based on conjugated polymers, e.g. poly [2-methoxy-5-(2'-ethyl hexyloxy)-1, 4-phenylene vinylene (MEH-PPV), which has resulted in further increase in the power conversion efficiency (PCE) of the cells [22]. MEH-PPV has been extensively used as a thin film in various optoelectronic devices such as organic light emitting diodes (OLEDs) due to its good solubility in various solvents, relatively low cost, and simple processing using spin coating [14, 23–26].

For the fabrication of the active layer in electronic devices based on solution processed conjugated polymers, spin coating is considered as the most reliable process [21, 27]. Recently, many researchers studied the effect of blending two conjugated polymers to enhance the performance of organic solar cells [14, 28]. This concept of combining the two polymers in photovoltaic PV devices can contribute significantly to the overall solar light absorption. However, despite the enormous progress made in the processing of organic solar cells, not many experimental analyses have been reported on the blending of poly[(9,9-dioctyl-2,7-divinylene)fluorenylene]-alt-co-(1,4-phenylene)] (PFO-MEH-PPV) with poly[3-(2-ethyl-isocyanato-octadecanyl) thiophene] (PECOD). In addition, there are few studies on the carrier mobility of spin-coated conjugated polymers used in optoelectronic devices, where the thickness of the blend layer ranges between 50 and 200 nm of almost all organic materials used in solar cells.

In order to achieve more satisfying results, it is pivotal that research is conducted towards better understanding of the dynamics of the charge carriers, in both pure and blended conjugated polymers in the active layer as this is one of the prime properties that govern the development of improved optoelectronic devices, such as organic solar cells based on such polymers. Moreover, the morphology of MEH-PPV films must be manipulated to fine-tune its response using different organic solvents, concentrations and spin speeds, to optimize the optical and electrical properties of the polymer films used in organic solar cells and LEDs [10, 11, 25]. In particular, MEH-PPV a conjugated polymer with exceptional optical and electrical properties is amenable to such optimization and as such is a promising candidate for applications in organic solar cells and light emitting diodes.

In this paper, a set of solar cells based on pure and blended PFO-MEH-PPV and PECOD as the active organic layer were fabricated. In order to investigate the optical properties of the polymeric thin films, the absorbance spectra were measured in the range 250–700 nm. PL spectra were studied for the pure and blended PFO-MEH-PPV and PECOD polymers dissolved in tetrahydrofuran (THF) and chlorobenzene (CB) and deposited with different concentrations/thicknesses on glass substrates. The cells were fabricated on indium-tin-oxide (ITO)-glass substrates used as top electrode.

In addition, the electrical characterizations of the various cells made of pure conjugated polymer and the roles of blending the two polymers were examined. The behavior of the current–voltage (I–V) characteristics for both pure polymer/blends and the conduction mechanism for each case are discussed and compared with the currently available conduction models and also its impact on the PCE of the fabricated solar cells.

2 Materials and methods

The PFO-MEH-PPV ADS128GE with PECOD ADS518PT conjugated co-polymers have a molecular weight of 270,000 and 152,000, respectively, supplied by (American Dye Source, Canada) and used as received. The molecular structures of the two polymers are given in Fig. 1a, b. The PFO-MEH-PPV and PECOD solutions were prepared, and the used solvent was a 1:1 ratio of CB and THF. To prepare the blend polymer films, a solution of 1:1 mix of the two polymeric solutions were deposited by spin coating onto the previously cleaned glass substrates followed by spectral characterization such as absorbance and PL. Each spin coating was performed for a spin time of 20 s. To measure the amount of ultra violet/visible (UV-Vis) light absorbed by the pure and blended polymeric active layer, the UV-Vis

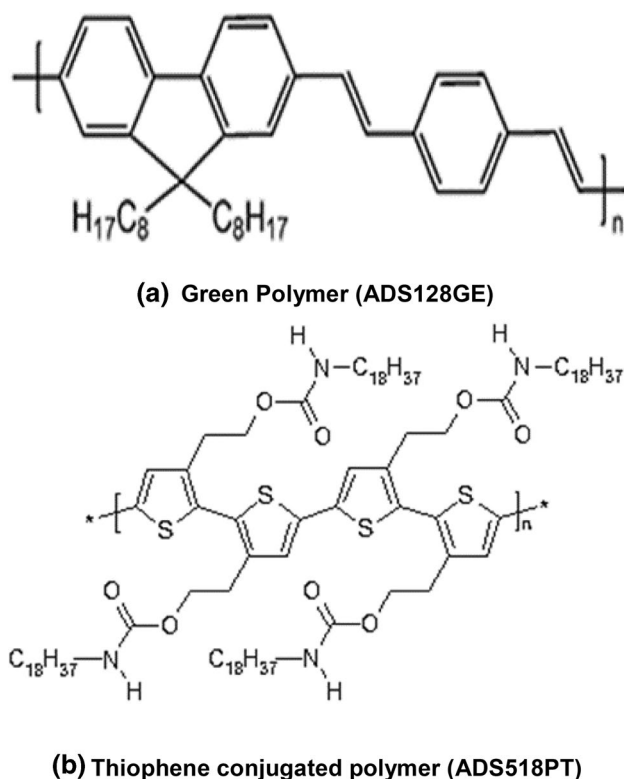


Fig. 1 Molecular structures of the two polymers

absorption spectra for the polymer films spin-coated on glass were obtained in the range of 300–700 nm by using Perkin Elmer lambda 950 UV–Vis spectrophotometer: scans were performed at a speed of 37 nm min⁻¹ with a bandwidth of 1 nm.

To study the behavior of the polymeric active layer molecules in the excited state, the fluorescence spectra were recorded using a Perkin Elmer LS-45 spectrofluorometer. The glass and ITO-coated glass substrates (Aldrich Co.) were cleaned in an ultrasonic bath with acetone, methanol, and deionized water then dried in high purity nitrogen. The ITO films have a low resistivity of $2.25 \times 10^{-4} \Omega \text{ cm}$, transmittance around 90% in the visible range, and thickness of 150 nm. For the polymeric layers, thickness measurements were conducted using a high performance Deck Tack 150 surface profiler from Veeco with a contact stylus profilometry.

The polymeric solar cells with various structures such as ITO/PFO–MEH–PPV/Ag, ITO/PECOD/Ag, and ITO/PFO–MEH–PPV: PECOD/Ag were fabricated by thermal evaporation of a thin layer (110 nm) of silver (Ag) metal on the top of the spin coated polymer layer via a mask at a base pressure of 10^{-6} Torr.

Figure 2 shows the schematic diagram of the fabricated solar cells, where the active layer is made of pure or blended conjugated polymers with PFO, PECOD, and PFO: PECOD, separately.

Furthermore, PL spectra well known as the intensity of radiation by the samples as a result of stimulation with incident light were studied. The PL spectra were recorded using a spectrofluorometer (Perkin Elmer LS-45) at room temperature.

Finally, the I–V characteristics curves of the fabricated solar cells were also collected at room temperature using a Keithly source meter model 2400 interfaced to a personal computer. The I–V measurements were repeated for a second time after maintaining the devices for a period of one

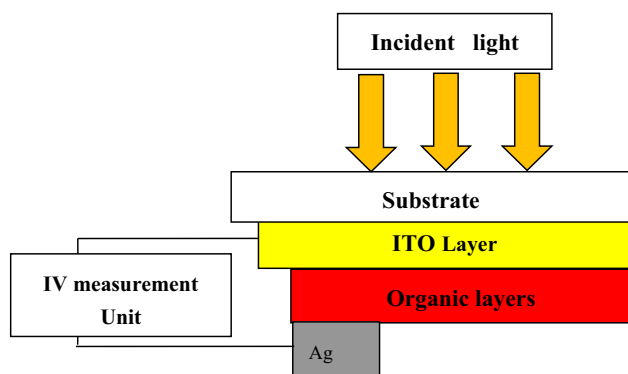


Fig. 2 Schematic diagram of the organic solar cell

month in the dark at room temperature in order to assess the accuracy of our results.

3 Results

3.1 Spectral properties

Prior to measure the spectral properties such as absorption and fluorescence of the polymeric layers, we examined the thickness of these layers for various solution concentrations and spin speeds. Figure 3 shows the spin speed and thickness of the film formed. The properties and combination of solvents mixtures have a crucial parameter in the performance of devices fabricated through the spin coating method [28–32]. The common solvent used was the mixture 1:1 of CB and THF because CB an aromatic solvent CB with a low evaporation rate dissolved PECOD and THF a non-aromatic solvent chloroform with a high evaporation rate dissolved GP well. The spin duration was 20 s for all layers made for this study. The concentration was 2 mg of polymer in 1 ml of solvent (2 mg/ml). The red line is for TCP, the green line is for GP, and the blue line is for the solution of 1:1 mixture of both TCP and GP.

The spin speed was varied to explore the optimum film thickness with the concentration solution used and examine whether the thickness of the thin film has any effect on absorption spectrum and fluorescence. It is clear that the

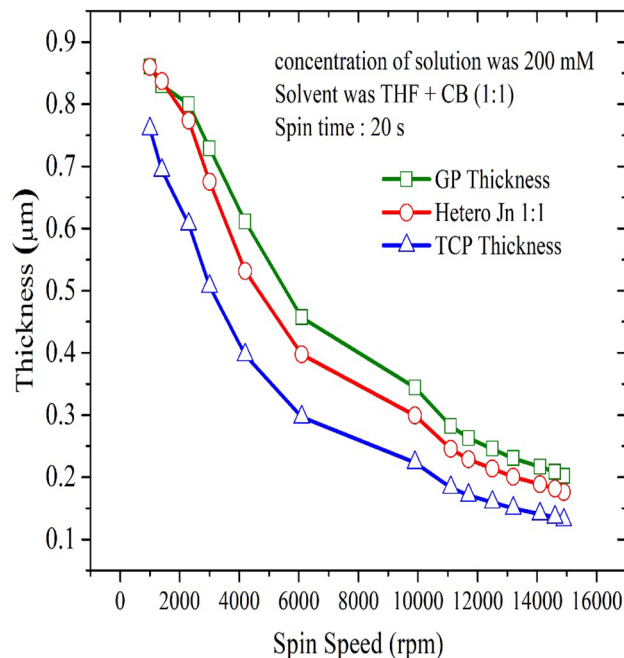


Fig. 3 Variation of the polymeric layers with the spin speeds

polymeric film gets thinner when the spin speed is increased for the three solutions, as in Fig. 3.

We conclude that the desired thickness of the film depends on the polymer solution concentration, solvent used, spin time, and spin speed. The thickness of the thin film is expected to affect the absorption spectra and fluorescence as well as charge separation, transport and collection. In similarity to our results, Li and co-authors reported that controlling the polymeric active layer thickness has resulted in an increased absorption and external quantum efficiency (EQE) of the solution processable polymer solar cells [30].

Figure 4 represents the absorbance spectra of the GP polymer recorded for various concentrations ranging from 0.07 to 0.75 mM. It was shown that only one peak was present at a wavelength of 420 nm for all the concentrations used, the peak was greatly enhanced by increasing the polymer concentration as observed in Fig. 4.

For the TCP polymer, Fig. 5 shows the absorbance spectra for the concentration ranging from 0.13 to 1 mM. The absorption peaks of the pure TCP are located one at 460 nm and at ~485 nm. The intensity of the peaks increases when the concentration of polymer increases while maintaining the same shape as observed in Fig. 5.

We expect to widen the absorption when the two constituent polymers GP and TCP are blended as depicted in Figs. 4 and 5 especially on the red wing of the band which will afford better capturing of sunlight. Such visible light absorption by the GP and TCP is critical to the performance of organic solar cells. For this reason, higher light-harvesting efficiency can lead to higher photocurrent in solar cells.

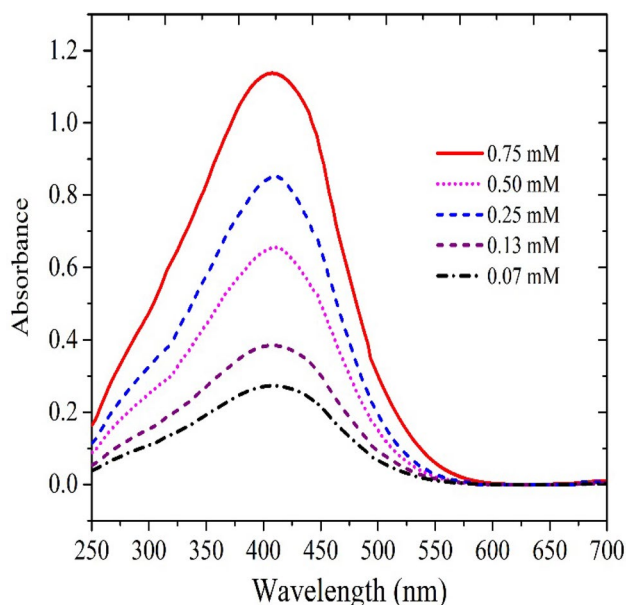


Fig. 4 Absorbance spectra versus wavelength of the GP polymer for the concentrations ranging from 0.07 to 0.75 mM

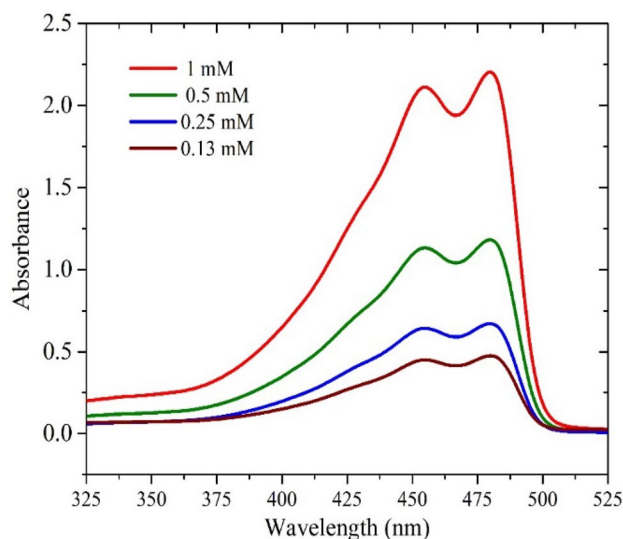


Fig. 5 Absorbance spectra versus wavelength for the TCP polymer for the concentration ranging from 0.13 to 1 mM

Similarly, this visible light harvesting may be enhanced in blended conjugated polymers through good design choice and thickness of the solar cell's active layer structure.

We concluded from Figs. 3, 4, and 5 that Photon propagation through a thin film plays an important role in determining the efficiency of the solar cells because the longer it propagates; the higher is the chance of exciting a molecule. Moreover, if the thickness is high and there can be two problems: (1) non-radiative recombination of excited electrons and (2) reabsorption of photons. The fluorescence of film will increase when the thickness increases. But after a critical thickness value, the fluorescence starts to reduce due to the reabsorption process of the conjugated-polymer films. Hence, we have chosen the optimal thickness of films by measuring the fluorescence peak intensity versus thickness of the film.

Figure 6 shows the relationship between the thickness and fluorescence intensity (peak) of the samples. The green squares are actual values, and green line is 4th order polynomial fitting for the green polymer. Similarly, the dark red and blue lines represent the TCP and mixed solution, respectively. Here, the fluorescence increases with the increase in thickness for a range, and any further increase in thickness reduces the fluorescence due to the reabsorption process. When the thickness was in the range of 0.26–0.37 μm , the fluorescence approached the maximum value, to be exact i.e., GP was 0.37 μm thick and the fluorescence intensity reached its maximum (600 a.u.). Similarly, fluorescence reached its maximum when TCP was 0.26 μm and hetero was 0.33 μm . In this study, we used the thickness range of 0.26–0.37 μm for producing the devices. Note that there is another local maximum in the response for all cases at a

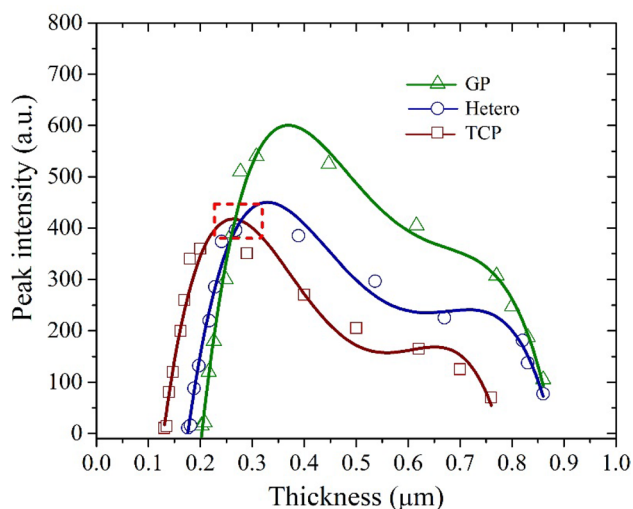


Fig. 6 Fluorescence intensity versus polymeric layer thickness

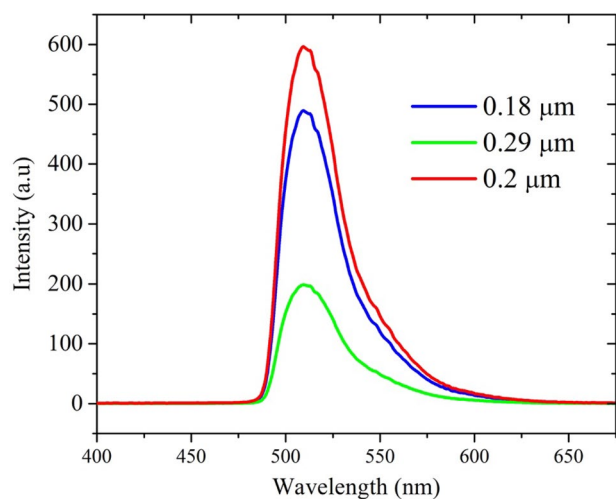


Fig. 7 Photo-luminescence of the GP polymer for the thickness ranging from 0.18 to 0.29 μm

thickness $\sim 0.72 \mu\text{m}$. The second maximum may be due to increased absorption of the incident light due to the larger depth.

For GP, the fluorescence intensity peak was observed at a thickness of $0.26 \mu\text{m}$; for TCP, it was at a thickness of $0.35 \mu\text{m}$; and for mixed polymer (GP:TCP), the maximum peak of fluorescence was observed at $0.33 \mu\text{m}$, when the wavelength of excitation was 355 nm .

Figure 7 shows the PL spectra of GP in the thickness range of $0.18\text{--}0.29 \mu\text{m}$. At $0.18 \mu\text{m}$, the PL increased up to $0.23 \mu\text{m}$, but for higher thickness, the PL decreased. One can observe also in Fig. 7 that the intensity of the PL spectra for GP increased when the thickness increased from 0.18 to $0.23 \mu\text{m}$. The fluorescence spectra have only one peak at around 510 nm , and the shape of the fluorescence remains

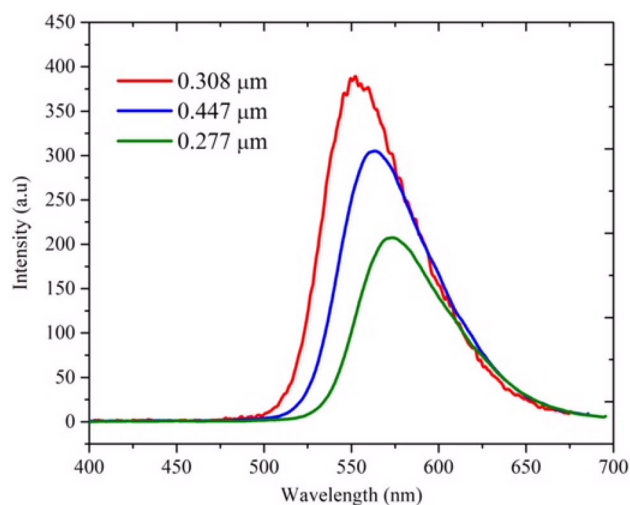


Fig. 8 Photo-luminescence spectra versus wavelength of the TCP films for the thickness ranging from 0.277 to $0.447 \mu\text{m}$

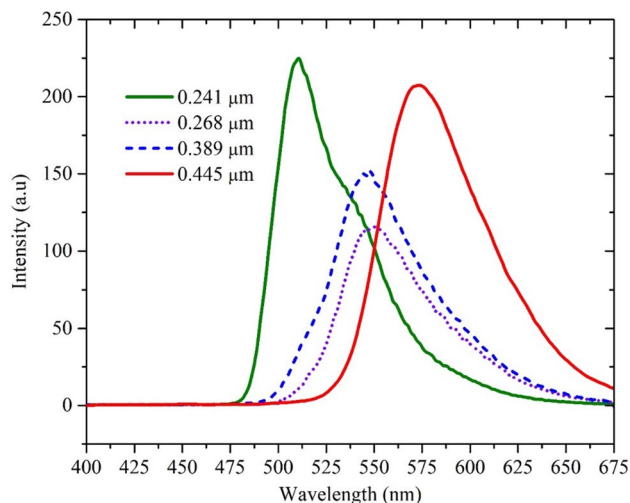


Fig. 9 Photo-luminescence spectra for TCP for thickness ranging from 0.241 to $0.455 \mu\text{m}$

the same although the thickness increased, but for thickness above $0.29 \mu\text{m}$, the PL decreased dramatically at the same wavelength (510 nm), when the wavelength of excitation was 355 nm .

Figure 8 shows the PL spectra of TCP in the range of $400\text{--}700 \text{ nm}$ for thickness ranging from 0.277 to $0.447 \mu\text{m}$.

The PL spectra of TCP increased for the thickness range of $0.277\text{--}0.308 \mu\text{m}$ with a slight shift in wavelength from 575 to 540 nm . For $0.447 \mu\text{m}$ thickness (TCP), the PL intensity decreases at a wavelength of 560 nm when the wavelength of excitation was 355 nm .

Figure 9 shows the PL spectra of TCP for a thickness range of $0.241\text{--}0.455 \mu\text{m}$. A dramatic variation can be seen

in PL due to energy transfer from GP to TCP. However, TCP dominates the PL spectra at higher thicknesses.

For TCP, the PL intensity peak was at 512 nm when the thickness was 0.241 μm, and it was 550 nm at a thickness of 0.268 μm. While for the thicknesses of 0.389 and 0.445 μm, the PL intensity peaks were at 540 nm and 580 nm, respectively. This clearly indicates the increase in PL intensity with the increase in polymer thickness when the wavelength of excitation was 355 nm.

3.2 Current–Voltage characterization

In order to investigate the solar cell performance, the I–V characteristics of the fabricated solar cells were measured using light intensity standardized at 100 mW/cm² with a spectral intensity distribution matching that of the sun on the earth’s surface.

I–V characterization of a set of eight different combinations of solar cell devices was performed. Here the devices are given the symbols D1–D8 respectively. The photovoltaic characteristics of the fabricated solar cells are represented

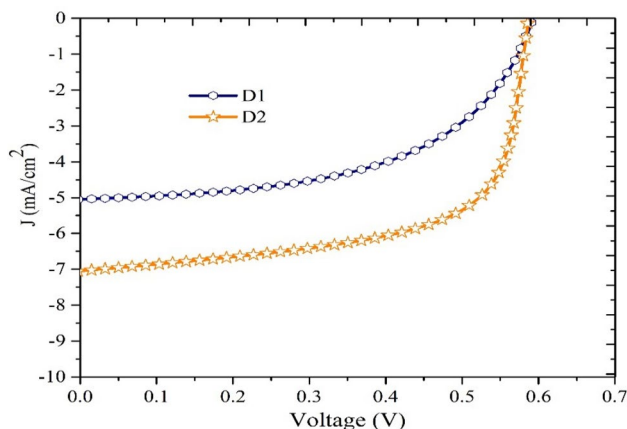


Fig. 10 I–V characteristics of the devices D1 and D2 based on GP

in Fig. 10, 11, 12 and 13 respectively, and also results are summarized in Table 1.

Figure 10 shows the IV characterization of GP devices D1 and D2. The following structures for the single layer’s (GP) devices D1 and D2 were used: [D1: ITO (150 nm)/GP (350 nm)/Ag (110 nm)], and D2: [ITO (150 nm)/GP (200 nm)/Ag (110 nm)]. It can be seen that D1 and D2 have an excellent fill factor (FF) of 57% and 45%, respectively. For D1, V_{oc} = 0.59 V and I_{sc} = 5 mA, and for D2, V_{oc} = 0.58 V and I_{sc} = 7 mA, which corresponds to an external PCE of 1.67% for D1 and 1.85% for D2. These measured parameters are in line with the values of pure polymeric solar cells reported earlier [25, 26]. Zhang and co-authors [25] achieved a PEC of 1.3% for polymer solar cells based on MEH–PPV and PCBM under illumination of AM 1.5. According to Sharma et al. [26], a PCE of 1.73% was achieved for organic solar cells based on MEH–PPV that improved to 1.95% after thermal annealing.

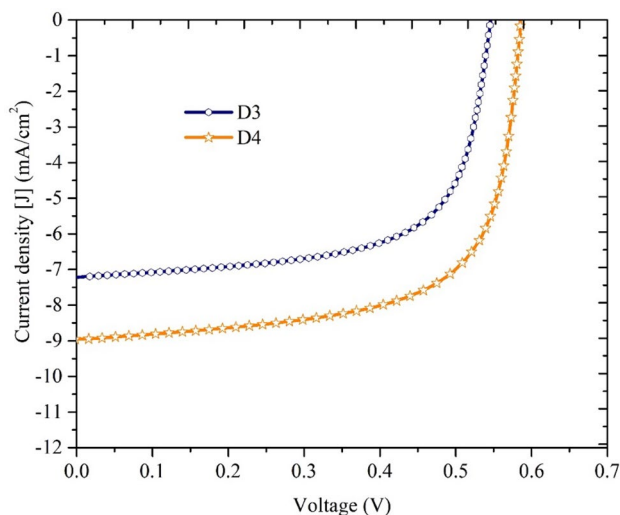


Fig. 11 I–V characteristics of the solar cells D3 and D4 based on TCP

Table 1 Various efficiencies of the fabricated solar cells

	V_{oc} (Volts)	I_{sc} (mA)	V_{max} (Volts)	I_{max} (mA)	Efficiency (%)	Input (mW/cm ²)	FF (%)	$V_{oc} \times I_{sc}$ (mW)
D1	0.59	5.01	0.44	3.77	1.67	100	0.57	2.94
D2	0.58	7.00	0.49	3.77	1.85	100	0.45	4.07
D3	0.55	7.20	0.45	5.90	2.62	100	0.67	3.91
D4	0.59	8.94	0.49	7.10	3.51	100	0.67	5.23
D5	0.58	8.34	0.46	6.15	2.82	100	0.59	4.80
D6	0.58	9.80	0.47	7.90	3.74	100	0.66	5.64
D7	0.67	11.44	0.52	8.58	4.46	100	0.58	7.68
D8	0.70	13.22	0.58	10.85	6.29	100	0.68	9.24

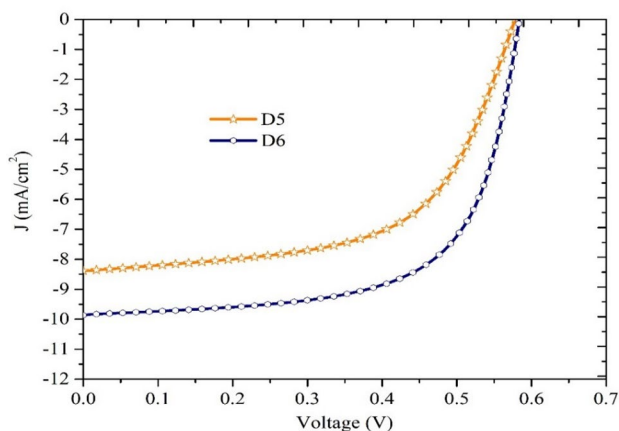


Fig. 12 Current density versus the voltage for cells D5 and D6

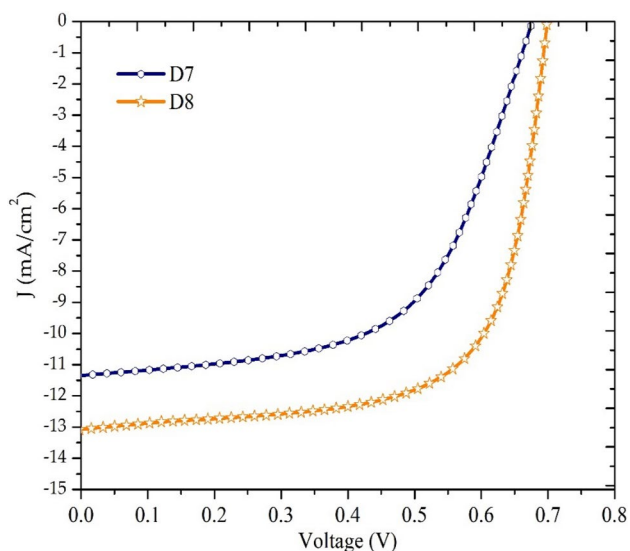


Fig. 13 The I–V characteristics of the D7 and D8 solar cells

Figure 11 shows the IV characterization of TCP devices D3 and D4. The following structure for the single layer's (TCP) devices D3 and D4 were used. D3: [ITO (150 nm)/TCP (450 nm)/Ag (110 nm)] and D4: [ITO (150 nm)/TCP (308 nm)/Ag (110 nm)]. D3 and D4 have an excellent FF of 67%. For D3, $V_{oc} = 0.55$ V and $I_{sc} = 7.20$ mA, but for D4, $V_{oc} = 0.59$ V and $I_{sc} = 8.94$ mA, which corresponds to an external PCE of 2.62% for D3 and 3.51% for D4. Castro and co-authors [27] reported an efficiency of 1.85% under 100 mW/cm^2 AM 1.5 illumination for solar cells based on MEH–PPV– C_{60} annealed at 180°C with the highest FF reaching 51.5%. However, in our case, the increase in the FF for D3 and D4 devices can be explained by the increase in charge carrier mobility, as well as the much smoother surface of the polymeric active layer that leads to better interfacial contact with the silver cathode [21, 22]. Similar

to our work, this latter effect based on blending two conjugated polymers, was also investigated by other researchers. According to Sharma and co-authors, the performance of organic photovoltaics is severely limited by low efficiencies, short lifetimes and low charge mobilities in polymers. This challenge can be met through the use of blended and layered heterojunctions as such morphologies can offer thicker and more absorbing polymer films [26].

Another approach to understand the conductivity of the active layer was reported by Kumar and his co-authors. They analyzed the energy diagram for the MEH–PPV conjugated polymer which is a p-type semiconductor having lowest unoccupied molecular orbital (LUMO) value of 3 eV and highest occupied molecular orbital (HOMO) value of 5.3 eV, and its use with CdTe nanoparticles. Adding the nanoparticles resulted in reducing the band gap of the polymer and in improving the power efficiency of the cells [4]. Recently, Mustapha and co-authors reported that adding quantum dots and graphene to the active layer of a solar cell based on MEH–PPV, has resulted in enhancing the electron mobility/transfer into the conjugated polymer. The incorporation of graphene led to a PCE of 6.88% for the (MEH–PPV: CdSe: 0.1 mg-graphene) cells, which is higher than the 4.11% for the cells without graphene [21].

According to Tongay and co-authors, the use of graphene in organic solar cells based on MEH–PPV, resulted in improved PCE of the organic solar cells as a result of higher electrical conductivity in the graphene's blended active layer [33] and the associated reduction of ohmic losses for the MEH–PPV. We believe that a further investigation needs to be done to explain this behavior and to measure the resistivity of the pure and blended polymer.

More recently, many research activities were focused on the use of polymer/polymer blend solar cells that utilize conjugated polymers as both an electron donor and an electron acceptor, because they have numerous potential advantages over conventional polymer/fullerene blend solar cells [1, 34–36].

In addition to that, Kim and co-authors reported that, an acceptor and a donor conjugated polymers are needed for tuning the optical, electronic, morphological, and mechanical properties of the blended polymeric films. Therefore, it is necessary to obtain polymer/polymer blends which can absorb a large fraction of solar light, leading to a large short-circuit photocurrent density (J_{sc}). Furthermore, the adjustment of the HOMO and LUMO levels of the donor and acceptor polymers allows the open-circuit voltage (V_{oc}) to increase above 1 V. This will harvest the way for a polymer which provides a continuous pathway for charge carrier transport, for wide ranges of donor and acceptor material blending ratios, and leading to a high FF [37].

Figure 12 shows the IV characterization of GP/TCP layer by layer devices D5 and D6. The following structure for the

double layer's devices D5 and D6 were used—D5: [ITO (150 nm)/TCP (450 nm)/GP (300 nm)/Ag (110 nm)] and D6: [ITO (150 nm)/TCP (300 nm)/GP (200 nm)/Ag (110 nm)]. D5 and D6 have an excellent FF of 59% and 66%, respectively. For D5, V_{oc} = 0.58 V and I_{sc} = 8.34 mA, and for D6, V_{oc} = 0.58 V and I_{sc} = 9.77 mA, which corresponds to an external PCE of 2.82% for D5 and 3.74% for D6.

Figure 13 shows the IV characterization of GP + TCP hetero-junction devices D7 and D8. The following structure for the hetero-junction layer's devices D7 and D8 were used—D7: [ITO (150 nm)/TCP + GP (390 nm)/Ag (110 nm)] and D8: [ITO (150 nm)/TCP + GP (280 nm)/Ag (110 nm)]. For D7, the device showed a V_{oc} of 0.67 V and an I_{sc} of 11.44 mA, with a good FF of 58%. For D8, the V_{oc} increased significantly to 0.7 V. Both I_{sc} and FF increased slightly compared with the D7 device. Upon the making hetero junction solar cell using thiophene polymer and PFO-co-MEH-PPV devices showed significantly enhanced I_{sc} of 12–14 mA. In addition, it gave a relatively high V_{oc} close to 0.7 V, and the PEC was 4.4% for D7 and 6.25% for D8. The theoretical limit for hetero junction solar cells efficiency was around 25%, the commercial minimal efficiency of any solar device was 10%, and here, we showed that simple open air solution processing of conjugated-polymer blends could achieve efficiency close to 7%, which is an encouraging sign for future research. Note that these solar cells performed well for over 3 days of continuous testing without any significant damage. However, more research is required to reach the maximum efficiency to that of the theoretical limit.

Figure 14 shows EQE versus wavelength for the best-performance cells measured at ambient room-temperature conditions. For the D2 device based on (GP) ADS128GE, the maximum EQE (around 80%) was obtained at wavelength of

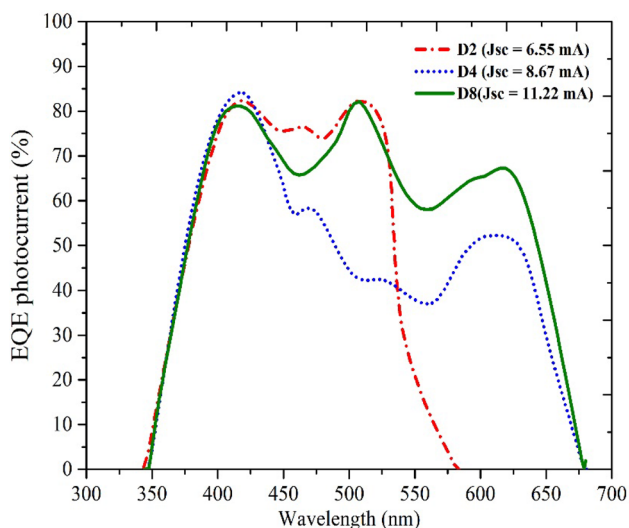


Fig. 14 External quantum efficiency of devices D2, D4 and D8

415 nm and 520, the calculated value of J_{sc} was 6.55 mA, then and a higher EQE (around 82%) was obtained at 415 nm, the calculated value of J_{sc} was 8.6 mA. For the D8 structure based on the blend (TCP + GP), the J_{sc} was 11.22 mA. The measured value of J_{sc} from IV measurement is different than J_{sc} calculated using IPEC, which could be due to the change in illumination area. The EQE was measured with an area of 0.5 cm² and IV measured with an area of 1 cm², but they approximately agree the result of each other. The drop-off in quantum efficiency at higher wavelengths is due to increased carrier emission in the device active layer, which reduces the leakage of light emitted at the interface between the ITO and the glass substrate. It is clear that the organic layer thickness and the blend concentration affected the efficiency of the solar cells. Recently, Kisslinger and co-authors [28] reported PCE of around 6% for hybrid solar cells based on conjugated polymer and CdSe quantum dots. In a similar way, CdSe quantum dots resulted in enhanced PCE up to 6.9% for solar cells based on MEH-PPV polymer [21]. This indicates that despite the advances made to improve PCE and performance of organic solar cells, further research work is necessary to optimize blend composition, device structure, and processing conditions to obtain higher PCE.

Sun and co-authors reported on the processing of organic solar cells with a high efficiency of 10.41% and the devices exhibit insensitivity of active layer thickness from 100 to 300 nm based on poly[(thiophene)-alt-(6,7-difluoro-2-(2-hexyloxy)quinoxaline)] (PTQ10) as a donor and by adding an *n*-OS IDIC as acceptor, they demonstrated an impressive PCE of 12.70% for an active layer thickness between 100 and 300 nm which is one of the highest PCE among the single-junction polymeric solar cells PSCs reported so far [38]. This combination of two materials is in similarity to our research in order to improve the PCE of the organic solar cells.

Table 1 represents the photovoltaic characteristics of the pure and blended conjugated polymers, where V_{oc} is the open circuit voltage, I_{sc} the short circuit current, FF is the ratio between the product of the maximum current (I_{sc}) and voltage (V_{oc}), and η is the efficiency of the solar cell. The active area of the solar cell devices was 1.25 cm × 1.28 cm = 1.6 cm².

To calculate the PCE, we used the Eq. (1):

$$\eta = \frac{V_{oc} I_{sc}}{P_{in}} \times FF \quad (1)$$

where P_{in} is the power of incident radiation per cm² and the FF was calculated by using the Eq. (2):

$$FF = \frac{I_{max} V_{max}}{V_{oc} I_{sc}} \quad (2)$$

The maximum incident power is given by the Eq. (3):

$$P_{max} = V_{oc} I_{sc} \times FF \quad (3)$$

The above I–V and EQE of devices of different combinations were compared, and based on their performance; we can conclude the following points. (i) The simplest, yet efficient device structure is the bulk heterojunction solar cells; and (ii) the layer thickness is an important factor, if the device thickness is large, then the efficiency is affected. Similarly, if the thickness is minimal, the efficiency is affected by disordered layer thickness and poor absorption of solar light. This new material blending proves to be the best among the organic solar cells, especially in conjugated polymer segment.

4 Conclusions

Single layer devices based on pure and blended conjugated polymers have been investigated. At optimal blend concentrations of PFO–MEH–PPV: PECOD, spectral properties showed PL covering a spectral range from 455 to 610 nm (minimum 50% of peak intensity). The performance of the organic solar cells was greatly improved by blending two conjugated polymers with a power efficiency of 6.25% and an EQE of 10.56% for the structure ITO/TCP + CP/Ag. In conclusion, we have shown that the blending of two conjugated polymers has resulted in improved PCE, and that the concentration of the blends and the thickness of the organic layers are critical in assessing the solar cell's performance. Finally, there is a great simplicity in the construction of solar cells based on solution-processable thin film conjugated polymers.

Further research work is required to optimize blend composition of the two conjugated polymers, thickness of organic layer, processing conditions and cell structure to obtain more improved electrical properties, PCE, and better performance of organic solar cells.

Acknowledgements This project was supported by King Saud University, Deanship of Scientific Research, Research Chairs. We thank Professor Munir H. Nayfeh at the University of Illinois for reading the manuscript and his valuable comments.

Author Contributions This work was carried out in collaboration between all authors. The idea was proposed by NM who was responsible for writing the draft of the manuscript. SP and MA carried out the experimental work, analysis and discussion of the results. Authors MA and SP reviewed the existing literature and placed the research objectives in perspective. All authors managed the reading, editing and approved the final manuscript.

Compliance with ethical standards

Conflict of interest The authors declare no conflict of interest.

References

1. C.R. McNeill, N.C. Greenham, Conjugated-polymer blends for optoelectronics. *Adv. Mater.* **21**, 3840–3850 (2009)
2. S. Barth, H. Bassler, Intrinsic photoconduction in PPV-type conjugated polymers. *Phys. Rev. Lett.* **79**, 4445–4448 (1997)
3. J. Li et al., Photovoltaic properties of MEH–PPV doped with new methanofullerene derivatives. *Synth. Met.* **137**, 1527–1528 (2003)
4. S. Kumar, T. Nann, First solar cells based on CdTe nanoparticle/MEH–PPV composites. *Mater. Res. Soc.* **19**, 1990–1994 (2009)
5. G. He, J. Liu, Y. Li, Y. Yang, Efficient polymer light-emitting diodes using conjugated polymer blends. *Appl. Phys. Lett.* **80**, 1891–1893 (2002)
6. A. Babel, S.A. Jenekhe, High electron mobility in ladder polymer field-effect transistors. *J. Am. Chem. Soc.* **125**, 13656–13657 (2003)
7. H. Sirringhaus, N. Tessler, R.H. Friend, Integrated optoelectronic devices based on conjugated polymers. *Science* **280**, 1741–1744 (1998)
8. J.H. Burroughs, D.C. Bradley, A.R. Brown, R.N. Marks, K.D. Mackay, R.H. Friend, P.L. Burn, A.B. Holmes, Light-Emitting Diodes Based on Conjugated Polymers. *Nature* **347**, 539–541 (1990)
9. A. J. Nozik, Quantum dot solar cells. *Physica E*, **14**, 115–120 (2002)
10. J. Liu, S.Y. Shi, L. Ma, Y. Yang, Device performance and polymer morphology in polymer light emitting diodes: the control of device electrical properties and metal/polymer contact. *J. Appl. Phys.* **88**, 605–607 (2000)
11. Y. Shi, J. Liu, Y. Yang, Device performance and polymer morphology in polymer light emitting diodes: the control of thin film morphology and device quantum efficiency. *J. Appl. Phys.* **87**, 4254–4263 (2000)
12. X. Deng, Light-emitting devices with conjugated polymers. *Int. J. Mol. Sci.* **12**, 1575–1594 (2001)
13. I.H. Campbell, B.K. Crone, Efficient, visible organic light-emitting diodes utilizing a single polymer layer doped with quantum dots. *Appl. Phys. Lett.* **92**, 043303/3 (2008)
14. H. Benten, D. Mori, H. Ohkita, S. Ito, Recent research progress of polymer donor/polymer acceptor blend solar cells. *J. Mater. Chem. A* **4**, 5340–5365 (2016)
15. D. Olzon-Dionysio, J.F.D. Chubaci, M. Matsuoka, R.M. Faria, F.E.G. Guimaraes, Ion beam assisted deposition of an organic light emitting diode electrode. *Surf. Coat. Technol.* **204**, 3096–3099 (2010)
16. S.C. Veenstra, J. Loos, J.M. Kroon, Nanoscale structure of solar cells based on pure conjugated polymer blends. *Prog. Photovolt.* **15**(8), 727–740 (2007)
17. T.-Q. Nguyen, J. Liu, B.J. Schwartz, Controlling interchain interactions in conjugated polymers: the effect of chain morphology on exciton–exciton annihilation and aggregation in MEH–PPV films. *J. Phys. Chem. B* **104**, 237–255 (2000)
18. A. Kraft, A.G. Grimsdale, A.B. Holmes, Electroluminescent conjugated polymers—seeing polymers in a new light. *Angew. Chem. Int. Ed.* **37**, 402–428 (1998)
19. S.A. Jenekhe, J.A. Osaheni, Excimers and exciplexes of conjugated polymers. *Science* **265**, 765–768 (1994)
20. X. Zhang, S.A. Jenekhe, Electroluminescence of multicomponent conjugated polymers. *Macromolecules* **33**, 2069–2082 (2000)
21. N. Mustapha, Z. Fekkai, A. Alkaoud, Enhanced efficiency of organic solar cells based on (MEH–PPV) with graphene and quantum dots. *Opt. Int. J. Light Electron Opt.* **127**, 2755–2760 (2016)
22. N. Mustapha, K.H. Ibnaouf, Z. Fekkai, A. Hennache, S. Prasad, A. Alyamani, Improved efficiency of solar cells based on

- BEHP-co-MEH-PPV doped with ZnO nanoparticles. *Opt. Int. J. Light Electron Opt.* **124**(22), 5524–5527 (2013)
23. A. Alyamani, K.H. Ibnaouf, O.S. Yassin, M.S. AlSalhi, Z. Fekkai, N. Mustapha, Spectral, electrical and morphological properties of spin coated MEH-PPV and cresyl violet blended thin films for a light emitting diode. *Opt. Int. J. Light Electron Opt.* **127**, 2331–2335 (2016)
 24. S. Hameed, P. Predeep, M.R. Baiju, Polymer light emitting diodes—a review on materials and techniques. *Rev. Adv. Mater. Sci.* **26**, 30–42 (2010)
 25. F.L. Zhang, M. Johansson, M.R. Andersson, J.C. Hummelen, O. Inganäs, O. Inganäs, Polymer solar cells based on MEH-PPV and PCBM. *Synth. Met.* **137**(1), 1401–1402 (2003)
 26. S.S. Sharma, K. Sharma, G. D. Sharma, Efficient bulk heterojunction photovoltaic devices based on modified PCBM. *Nanotechnol. Rev.* **4**(5), 419–428 (2015)
 27. F. Araujo de Castro, J. Heier, F. Nuesch, R. Hany, Origin of the kink in current-density versus voltage curves and efficiency enhancement of polymer-C60 heterojunction solar cells. *IEEE J. Sel. Top. Quantum Electron* **16**(6), 1690–1699 (2011)
 28. R. Kisslinger, W. Hua, K. Shankar, Bulk heterojunction solar cells based on blends of conjugated polymers with II–VI and IV–VI inorganic semiconductor quantum dots. *Polymers* **9**(2), 35–63 (2017)
 29. K. Norrman, A. Ghanbari-Siahkali, N. Larsen, Studies of spin-coated polymer films. *Annu. Rep. Prog. Chem. C* **101**, 174–201 (2005)
 30. G. Li, V. Shrotriya, J. Huang, Y. Yao, T. Moriarty, K. Emery, Y. Yang, High-efficiency solution processable polymer photovoltaic cells by self-organization of polymer blends. *Nat. Mater.* **4**, 864–868 (2005)
 31. F. Zhang, K.G. Jespersen, C. Bjoerstroem, M. Svensson, M.R. Andersson, V. Sundström, K. Magnusson, E. Moons, A. Yartsev, O. Inganaes, Influence of solvent mixing on the morphology and performance of solar cells based on polyfluorene copolymer/fullerene blends. *Adv. Funct. Mater.* **16**, 667–674 (2006)
 32. Y. Yao, J. Hou, Z. Xu, G. Li, Y. Yang, Effects of solvent mixtures on the nanoscale phase separation in polymer solar cells. *Adv. Funct. Mater.* **18**, 1783–1789 (2008)
 33. S. Tongay, K. Berke, M. Lemaitre, Z. Nasrollahi, D.B. Tanner, A.F. Herbard, B.R. Appleton, Stable hole doping of graphene for low electrical resistance and high optical transparency. *Nanotechnology* **22**, 42570–42571 (2011)
 34. S.C. Veenstra, J. Loos, J.M. Kroon, Nanoscale structure of solar cells based on pure conjugated polymer blends. *Prog. Photovolt. Res. Appl.* **15**, 727–740 (2007)
 35. C. R. McNeill, Morphology of all-polymer solar cells. *Energy Environ. Sci.* **5**, 5653–5667 (2012)
 36. A. Facchetti, Polymer donor–polymer acceptor (all-polymer) solar cells. *Mater. Today* **16**, 123–132 (2013)
 37. T. Kim, J.H. Kim, T.E. Kang, C. Lee, H. Kang, M. Shin, C. Wang, B. Ma, T.S. Kim, B.J. Kim, U. Jeong, Flexible, highly efficient all-polymer solar cells. *Nat. Commun.* **6**, 8547–8555 (2015)
 38. C. Sun, F. Pan, H. Bin, J. Zhang, L. Xue, B. Qui, Z. Wei, Z.G. Zhang, Y. Li, A low cost and high performance donor material for polymer solar cells. *Nat. Commun.* **9**(1), 1–10 (2018)

Publisher's Note Springer Nature remains neutral with regard to jurisdictional claims in published maps and institutional affiliations.